Gap formation in the transitional and pre-transitional disk: a model of dust filtration in the presence of coagulation and fragmentation

ISIMA student: Munan Gong
Advisor: Pascale Garaud
Collaborators: Christoph Olczak, Fazana Meru

September 17, 2011

Abstract

The transitional disks around young stars are protoplanetary disks with inner holes that are relatively empty of small dust grains, as inferred from the excess of far-infrared emission in their spectral energy distribution (SED)(Espaillat et al. 2007,2010). Recently, a new class of 'pre-transitional disks' are identified as exhibiting substantial emission from an optically thick inner disk separated from an optically thick outer disk by an optically thin gap(Espaillat et al. 2010). One plausible model for gap opening in these disks is by multiple giant planets(Zhu et al. 2011). However, two major problems remain to be solved. Firstly, micron-sized dust grains are not removed efficiently enough from the giant planet's gap to explain the observed low disk emission at near/mid-infrared wavelengths. Secondly, the presence of multiple Jupiter mass planets in resonance is not likely in standard disk models. We have developed a simple but robust coagulation-fragmentation model showing that piled-up material at the outer gap edge acts as a very efficient filter for micron-sized grains. Its reduction of the particle flow by two orders of magnitude provides excellent agreement with observational data. We can also produce high local surface density of particles at the outer edge of the gap, which may trigger planet formation in the outer disk.

1 Introduction

The formation of the transitional disks – protoplanetary disks with large holes of few to tens of AU as inferred from their SED – is still puzzling. Various models have been proposed to explain the relative scarcity of dust in the inner holes among which two seem to be most plausible: photoevaporation by the central star(Alexander & Armitage 2007, 2009) and gap formation by giant planets(Rice et al. 2006, Zhu et al. 2011).

However, photoevaporation models have difficulties at explaining two problems: the high accretion rate in some transitional disks(Espaillat et al. 2007) and the recently identified pre-transitional disks that show substantial emission from the inner most disk parts(Espalliat et al. 2010). As a result, gap opening by planets gained more and more attention. The presence of multiple gas giants(Zhu et al. 2011) succeed in reproducing the high accretion rate and disk structure in the pre-transitional disks, but it raises another major problem: micron-sized grains are not removed efficiently enough from the giant planet's gap to explain the observed low disk emission at near/mid-infrared wavelengths. Moreover, the formation of multiple gas giants in resonance itself is not likely in standard disk models. One possible mechanism to overcome these problems is the filtration effect(Rice et al. 2006) at the outer edge of the gap opened by a gas giant, which traps the grains coming in from the outer disk. This also increases the local particle density,and could in principle trigger another generation of planet formation.

Taking the idea of the filtration effect, we developed a 'one-box' model to probe more into the evolution of dust particles, considering the radial and vertical particle dynamics in the presence of coagulation and fragmentation. The derivation of the model is presented in section 2. The model parameters and initial condition are listed in section 3. Section 4 and 5 present the numerical results of the fiducial model, and an exploration of parameter space respectively. The conclusion and discussion of this work are presented in section 6 .

2 Model Setup: 'One-box' Model

2.1 General Methodology

When a Jupiter mass planet is formed in the gas disk around a solar type-star, tidal interactions between the planet and the disk open a gap around its orbit. At the outer edge of the gap, the pressure gradient is positive due to the increase of gas surface density, while far beyond the gap, the pressure gradient in the disk is negative due to the drop of gas surface density and temperature. The planet thus produces a local pressure maximum beyond its orbit, where the dust particles flowing in from the outer disk can be trapped and collide with each other. We investigate this system in a 'one-box' model, where the 'box' is located near the local pressure maximum, and assume that the dust and gas properties are uniform in the 'box', which is a good approximation if the 'width' if the box is relatively thin. We consider the dust particles flowing in and out of the 'box' in the presence of coagulation and fragmentation, by solving coupled ODEs for evolution of dust and gas.

2.2 Evolution of the Gas Disk

In the following, we always assume that the gas disk evolves independently of the dust, which is only true if the dust-to-gas ratio is substantially below unity. The standard evolution equation for gas surface density Σ of a thin Keplerian disk is

$$\frac{\partial \Sigma}{\partial t} + \frac{1}{r}\frac{\partial}{\partial r}(ru\Sigma) = 0, \tag{1}$$

where u is the radial velocity of gas in disk due to the viscous angular momentum transfer along the radial direction:

$$u = -\frac{3}{r^{1/2}}\frac{\partial}{\partial r}(r^{1/2}\nu_t\Sigma), \tag{2}$$

and r is the radius. The gas viscosity ν_t is mainly a result of turbulence, and modeled using the standard α-model:

$$\nu_t = \alpha_t c_s h = \alpha_t\sqrt{\gamma}\Omega_k h^2, \tag{3}$$

where c_s is the local sound speed and h is the local disk scale-height. Assuming that the gas temperature T_g can be written as a simple power law,

$$T_g = T_{g_{AU}}(\frac{r}{AU})^{-1/2}, \tag{4}$$

where AU is one astronomical unit, the disk scale height is:

$$h = h_{AU}(\frac{r}{AU})^{5/4}. \tag{5}$$

Then equation (1) has a similarity solution (Hartmann et al.1998):

$$\Sigma(r,t) = \frac{M_d(0)}{2\pi r R_1}\frac{1}{T^{3/2}}e^{-(r/R_1)/T}, \tag{6}$$

where

$$T = \frac{t}{t_s} + 1, \quad t_s = \frac{1}{3}\frac{R_1}{\nu_t(R_1)}, \tag{7}$$

where R_1 is a radial scale factor and $M_d(0)$ is the initial disk mass. The mass accretion rate of gas $\dot{M}_g$ is then given by

$$\dot{M}_g(r,t) = 3\pi\nu_t(r)\sigma(r,t) \tag{8}$$

$$= \frac{M_d(0)}{2t_s}\frac{1}{T^{3/2}}e^{-(r/R_1)/T}(1 - \frac{2(r/R_1)}{T}) \tag{9}$$

$$= \dot{M}_g(0)\frac{1}{T^{3/2}}e^{-(r/R_1)/T}(1 - \frac{2(r/R_1)}{T}), \tag{10}$$

where $\dot{M}_g(0)$ is the initial mass accretion rate into the central star at $r = 0$. As the disk evolves, the angular momentum is transported outward and the

disk expands, while the total disk mass decreases due to accretion. The mass flux changes sign at radius R_t:

$$R_t = R_1 \frac{T}{2}. \tag{11}$$

Generally speaking, we are only interested in the gas flow into the box. As long as the box is much is much closer in than R_t, then from (10) we see that $\dot{M}_g$ is constant with r, and has gas (and consequently dust particles too) moving inward.

2.3 Particle-Size Distribution Function

In this model, we adopt the assumption of Garaud 2007, that the size distribution of particles always follows a power law:

$$\frac{\mathrm{d}n_{max}}{\mathrm{d}s_{max}} = \begin{cases} \frac{n_{max}}{s_{max}} \left(\frac{s}{s_{max}}\right)^{-3.5}, & s \in [s_{min}, s_{max}] \\ 0, & \text{otherwise} \end{cases} \tag{12}$$

where the size of the biggest body s_{max} and the number density n_{max} are both allowed to vary with time. The power law distribution over a large size range is a common result in the equilibrium between coagulation and fragmentation, from theory and experiment of particle collisions, and observation of Kuiper belt objects and asteroids. The coagulation and fragmentation processes are still quite uncertain, and all factors such as material strength, porosity and velocity dispersion can lead to different power law indices. Moreover, observations show that the index can change at the very high-mass end. The typical value for the power law index is between $[-3, -4]$, and we adopt -3.5 here. Within this assumption, n_{max} is directly related to the surface density of particles Σ_p

$$n_{max} = \frac{\Sigma_p}{2m_{max}\sqrt{2\pi}h_p}, \tag{13}$$

assuming that ρ_p has a Gaussian profile across the disk with scale-height h_p. The explicit expression for h_p,the particle scale-height, is given below.

2.4 Particle Dynamics

2.4.1 Turbulent Induced dynamics

Particles are coupled with the gas through frictional drag. For particles much smaller than the mean free path of gas $\lambda = \frac{1}{n\sigma}$ (Epstein regime), where n is the number density, and σ is the cross section of gas molecules, the drag forces originate from random collisions with the gas molecules. The time-scale within which the particles stop relative to the gas is

$$\tau(s) = \frac{s\rho_s}{\rho c_s}, \tag{14}$$

where ρ_s and ρ are the solid and gas mass density respectively. In order to evaluate the effect of gas drag on particles of different sizes, it is useful to define the Stokes number (Weidenschilling 1977)

$$St(s) = \frac{\tau(s)}{\tau_d}, \tag{15}$$

where $\tau_d = 2\pi/\Omega_k$ is the orbital time. Very small particles with $St(s) \ll 1$, are well-coupled with the gas, while very big ones($St(s) \gg 1$) barely feel the gas drag. The imperfect coupling between gas to particles leads to differential motion between the two, and different structures for the gas and particle disk.

2.4.2 Vertical Disk Structure

In the vertical direction of the disk, grains settle down to the mid-plane under the gravity of central star, but are also mixed upward by turbulent diffusion. Following the work of Garaud 2007, the size-averaged turbulent diffusivity D_t is related to ν_t by the effective Schmidt number Sc_{eff}

$$D_t(s) = \frac{\nu_t}{Sc_{eff}} \tag{16}$$

$$Sc_{eff} = \frac{\sqrt{St_{max}}}{\arctan(\sqrt{St_{max}})}, \tag{17}$$

where $St_{max} = St(s_{max})$ is the Stokes number for the maximum sized particle. The particle scale-height h_p can be obtained in the equilibrium state, and written as

$$h_p = h\left(1 + \frac{2\pi}{3}\frac{St_{max}Sc_{eff}}{\alpha_t\sqrt{\gamma}}\right). \tag{18}$$

2.4.3 Radial Drift of Particles

Feeling the gas drag, the particles exchange angular momentum with the gas, moving radially at the velocity (Weidenschilling 1977)

$$u_p(s) = \frac{u}{4\pi^2 St^2(s) + 1} - 2\eta v_k \frac{2\pi St(s)}{4\pi^2 St(s) + 1}, \tag{19}$$

where $u = \dot{M}_g/2\pi r\Sigma$ is gas radial velocity, v_k is the Keplerian orbital velocity, and

$$\eta = -\frac{1}{2}\frac{h^2}{r^2}\frac{\partial \ln p}{\partial \ln r}, \tag{20}$$

is related to the gas pressure gradient. Integrating equation (19) over all sizes, the mass averaged radial velocity is (Garaud 2007)

$$u_p = uI(\sqrt{2\pi St_{max}}) - 2\eta v_k J(\sqrt{2\pi St_{max}}), \tag{21}$$

where the functions

$$I(x) = \frac{\sqrt{2}}{4x}[f_1(x) + f_2(x)], \tag{22}$$

$$J(x) = \frac{\sqrt{2}}{4x}[-f_1(x) + f_2(x)], \tag{23}$$

with

$$f_1(x) = \frac{1}{2}\ln\left(\frac{x^2 + x\sqrt{2} + 1}{x^2 - x\sqrt{2} + 1}\right), \tag{24}$$

$$f_2(x) = arctan(x\sqrt{2} + 1) + arctan(x\sqrt{2} - 1). \tag{25}$$

2.5 Dust Filtration

Within the gap, the gas undergoes gravitational interactions with the planet, inducing a much more vigorous angular momentum transport. We model this with

$$\alpha_t(r) = \alpha_{t_0} + \frac{\alpha_{t_1} - \alpha_{t_0}}{2}\left(1 + \tanh\left(\frac{r_{planet} - r}{\Delta r}\right)\right), \tag{26}$$

where r_{planet} is the semi-major axis of the planet, Δr is the width of the gap edge, and α_{t_0} and α_{t_1} are the turbulent parameter in the gap and the outer disk. As a result, ν_t within the disk is

$$\nu_t(r) = \alpha_t(r) c_s h \tag{27}$$

$$= \alpha_{t_0} c_s h \cdot \frac{\alpha_t(r)}{\alpha_{t_0}} \tag{28}$$

$$= \nu_{t_{AU}} \frac{r}{AU} \cdot \frac{\alpha_t(r)}{\alpha_{t_0}}. \tag{29}$$

The first term in equation (29) is the viscosity without a gap, and the second term models the effect of the gap.

Δr can be evaluated from advection-diffusion balance

$$\Delta r = \frac{\nu_t}{u} = \frac{\dot{M}_g/3\pi\Sigma}{\dot{M}_g/2\pi r\Sigma} = \frac{2}{3}r \tag{30}$$

This is reasonably consistent with the results of Zhu et al. 2011 and Crida et al. 2006.

In this model, the box centered around the outer edge of the gap, located at $r = r_{box}$ with

$$r_{box} = r_{planet} + \Delta r = \frac{5}{3} r_{planet}. \tag{31}$$

This assumes the local density maximum overlaps the local pressure maximum. Considering that the temperature drops at outer radius, the local pressure maximum should actually be closer in.

Combining equation (8) and (29), we get the gas density profile at across the gap

$$\Sigma_{gap} = \frac{\dot{M}_g}{3\pi\nu_{t_{AU}} \frac{r}{AU} \cdot \frac{\alpha_t(r)}{\alpha_{t_0}}} \tag{32}$$

The increase of surface density at the gap edge creates a region where η is negative, causing the particles to gain angular momentum and move outward to the local pressure maximum. However, very small grains remain well-coupled with the gas and flow inward. This acts like a filter for the particles coming in from the outer disk and only the larger particles can be trapped.

In equation (19), let $u_p = 0$ and in the limit $St \ll 1$, s_{trap} can be solved as

$$s_{trap} = \frac{1}{4\pi\sqrt{2\pi}} \left(-\frac{1}{\eta_{box}}\right) \frac{\dot{M}_g}{\rho_s r_{box} v_k}, \tag{33}$$

where η_{box} by definition is calculated using equation (20), where the gas pressure is relate to Σ_{gap} in equation (32):

$$\eta_{box} = -\frac{1}{2}\frac{h_{box}^2}{r_{box}^2}\left(\frac{3}{4}\frac{\alpha_{t_1} - \alpha_{t_0}}{\alpha_{t_0}} - \frac{11}{4}\right). \tag{34}$$

2.6 Surface Density Evolution of Particles

The conservation of mass of particles in the 'box' is written as

$$\dot{M}_p^{box} = \dot{M}_p^{in} - \dot{M}_p^{out} \tag{35}$$

The mass inflow of small particles coming from the outer disk is

$$\dot{M}_p^{in}(t) = Z^{in}\dot{M}_g(r_{box}, t), \tag{36}$$

where Z^{in} is dust to gas ratio in the outer disk. The mass outflow is calculated by considering only the particles in the 'box' which are smaller than s_{trap}, and therefore move with the gas

$$\dot{M}_p^{out} = 2\pi r_{box} u \Sigma_p (s < s_{trap}) \tag{37}$$

$$= \frac{\dot{M}_g}{\Sigma}\Sigma_p\sqrt{\frac{s_{trap}}{s_{max}}}. \tag{38}$$

The last term in equation (37) comes from the integration over the -3.5 power law distribution of particle sizes.

Although the particles tend to be trapped at the local pressure maximum, they are not contained in an infinitely narrow region, because they diffuse due to turbulent mixing. The width of this region is determined by advection-diffusion balance similarly with equation (30), but the diffusion

coefficient and velocity should be that of particles averaged over all sizes in equation (16) and (21)

$$\Delta r_p = \frac{D_t}{u_p}. \tag{39}$$

As the particles grow bigger, they become less affected by the turbulence diffusion and more concentrated at the local pressure maximum. The biggest ones barely feel the turbulence and stay where they are formed. We model this effect by varying the 'thickness' of the 'box' while conserving the total mass M_p in the box. Therefore, the particle surface density in the box is given by

$$\Sigma_p = \frac{M_p}{2\pi r_{box} \Delta r_p}. \tag{40}$$

2.7 Particle Growth

Here we follow the Garaud 2007 paper in the treatment of particle growth. The number density of particles in a given size range increases by fragmentation of bigger bodies and decreases by their coagulation with other particles. Assuming the time-scale for the balance of coagulation and fragmentation is shorter than other dynamical time-scales in the 'box', the size distribution follows a fixed power law, and the size of the biggest particle grows with time. The evolution of s_{max} follows the standard coagulation equation

$$\frac{\mathrm{d}m_{max}}{\mathrm{d}t} = \int_{s_{min}}^{s_{max}} \frac{\mathrm{d}n}{\mathrm{d}s}(s') m s' \Delta v(s_{max}, s') A(s_{max}, s') \epsilon \mathrm{d}s'. \tag{41}$$

The relative velocity of particles of different sizes Δv is assumed to be driven by turbulence. The collisional cross section A here is the geometric cross section, for in our model where $r > 30AU$, particles never grow big enough for the gravitational focusing to become important. In this case, equation (41) can be written as

$$\frac{\mathrm{d}s_{max}}{\mathrm{d}t} = \frac{\Sigma_p}{\rho_s} \sqrt{2\pi\gamma} \frac{h}{h_p} \sqrt{\frac{\alpha_t St_{max}}{1 + 64 St_{max}^2 (2 + 2.5 St_{max}^{-0.05})^{-2}}} \frac{\epsilon}{\tau_d}. \tag{42}$$

The sticking efficiency ϵ is a constant here, and can be seen as an average sticking efficiency over all sizes and velocities. This is treated as an uncertain free parameter.

2.8 Dust to Gas Ratio in the Gap

Since only particles smaller than s_{trap} are allowed to pass through the pressure maximum, the dust-to-gas ratio in the gap is given by

$$Z^{out} = \frac{\Sigma_p^{box}(s < s_{trap})}{\Sigma^{box}} \tag{43}$$

$$= \frac{\Sigma_p^{box}\sqrt{s_{trap}/s_{max}}}{\Sigma^{box}} \frac{\Delta r_p}{\Delta r}. \tag{44}$$

The last term in equation (44) $\Delta r_p/\Delta r$ models the spreading of the smaller particles, via advection-diffusion balance, in a wider area while the big ones concentrates around the local pressure maximum.

2.9 Numerical Procedure

We solve two coupled ODEs, equation (35) and (42), for the evolution of particle mass and size distribution in the 'box', using the fourth order Runge-Kutta method. The dust-to-gas ratio in the gap is deduced from the diagnostic equation (44).

3 Model Parameters and Initial Conditions

3.1 Model Parameters

The parameters used in the fiducial model are listed in Table 1, including stellar parameters, disk parameters, and grain parameters.

Table 1: Fiducial Model Parameters

Parameter	Symbol	Value
Stellar mass (M_{solar})	M_*	1
Initial disk mass (M_{solar})	$M_d(0)$	0.1
Initial gas accretion rate onto the central star (M_{solar}/yr)	$\dot{M}_g(0)$	10^{-8}
Disk aspect ratio at 5AU	$(\frac{h}{r})_{5AU}$	0.06
Turbulent parameter in the outer disk	α_{t_0}	0.001
Turbulent parameter in the gap	α_{t_1}	0.01
Dust-to-gas ratio in the outer disk	Z^{in}	0.01
Semi-major axis of planet (AU)	r_{planet}	30
Adiabatic index	γ	1
Solid mass density (g/cm^3)	ρ_s	1
Sticking efficiency	ϵ	0.1

The stellar and disk parameters are taken as the typical values for pre-transitional disks in Espaillat et al. 2010. The position of the planet $r_{planet} = 30AU$ gives the location of the 'box' $r = 50AU$, which is the typical outer

edge of the gap. The adiabatic index $\gamma = 1$ is for an isothermal disk in vertical direction. The solid mass density should depend on radius and particle size in principle, but is taken as a constant here for simplicity. We choose $\rho_s = 1 g/cm^3$ for these are icy grains coming from the outer disk, and even for more porous or denser silicate grains, the variation of density is within a factor of a few, so this may not be a bad approximation. The sticking efficiency is the most uncertain parameter in our model, which can be seen as the average sticking efficiency for the growth of the biggest particle over all particle sizes and collisional velocities. We start with $\epsilon = 0.1$, and later carry out a parameter search.

3.2 Initial Conditions

The initial conditions used in this model are listed in Table 2. In fact, later we will show that s_{max} and M_p grow significantly after $\sim 1 Myr$, and the result is relatively insensitive to the initial conditions.

Table 2: Fiducial Model Initial Conditions

Parameter	Symbol	Value
Maximum particle size (cm)	s_{max_0}	0.1
Surface density of particles (g/cm^2)	Σ_{p_0}	$Z^{in}\Sigma$
Total particle mass in the box	M_{p_0}	$2\pi r_{box}\Sigma_{p_0}\Delta r_p(s_{max_0})$

4 Results in the Fiducial Model

The fiducial model was integrated for $1 Myr$. Figure 1 shows the evolution of mass and surface density in the 'box'. Figure 2 shows the size growth of the biggest particle and the change of the 'width' of the 'box'. Figure 3 shows the properties of gas background: accretion rate of gas at $r = 0, r_{box}$ and the gas surface density $\Sigma_g(r = r_{box})$. Finally, Figure 4 shows the depletion of metallicity in the outflow and the evolution of s_{trap} due to the evolution of gas background.

4.1 Evolution of Particle surface density

As can be seen from Figure 1, after $1 Myr$, several Earth masses solids are trapped at the outer edge of the gap. The particle surface density increases rapidly at first, and then slows down after $\sim 0.5 Myr$, as a result of the concentration of particles due to size growth shown in figure 2. Finally the surface density of particles is increased locally by a factor of ~ 100, comparable to the surface density of gas.

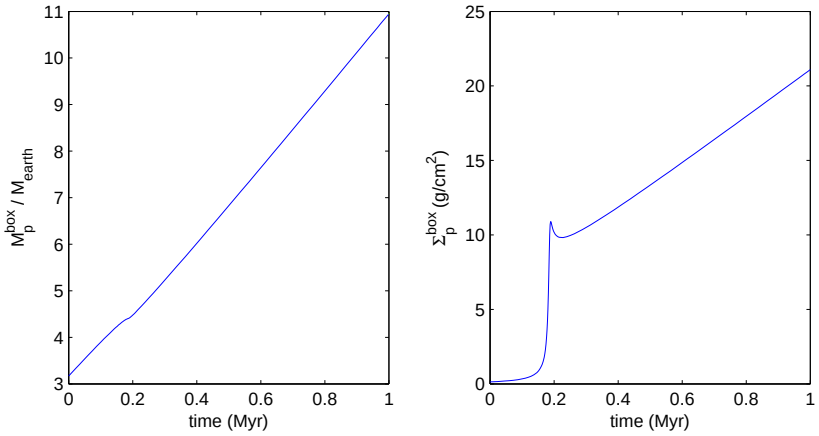

Figure 1: The evolution of total particle mass M_p^{box} (*left*) and the surface density of particles Σ_p^{box} (*right*) in the 'box'.

4.2 Particle Growth

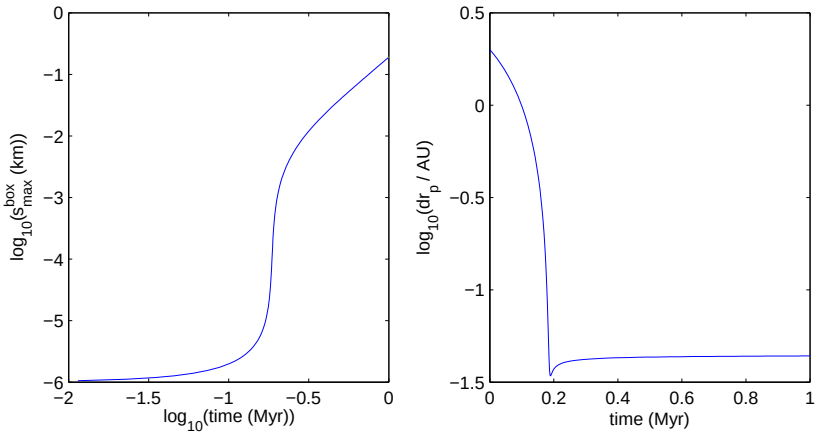

Figure 2: The size of the biggest particle s_{max}^{box} (*left*) and the effective 'box width' Δr_p (*right*).

Figure 2 shows that as the result of filtration and particle growth, $\sim 0.1AU$ belt of $\sim 100m$ planetesimals forms beyond the orbit of the planet $1Myr$ after its formation. In the classical planet formation scenario, this area should be a much more favorable place for the formation of another generation of planets in the outer disk than the standard disk model.

As expected from equation (42), the growth rate of the particles is proportional to the local particle surface density, and Figure 1 and 2 show that they both have a period of rapid increase, which correspond to the sharp

decrease of Δr_p at $t \sim 0.5 Myr$. This effect can be inferred from equation (39) and (19): when s_{max} grows to a size ($\sim$ $1cm$ in the fiducial model) that $St_{max} \sim 1$, the particle radial velocity u_p reaches its peak, where Δr_p is minimum. As s_{max} continue to grow, in the limit of $St_{max} \gg 1$ and $u \ll \eta v_k$, equation (17) and (21) equals to

$$Sc_{eff} = \frac{\pi}{2}\sqrt{St_{max}}, \quad u_p = -2\eta v_k \frac{\sqrt{\pi}}{4\sqrt{St_m ax}} \quad (St_{max} \gg 1), \tag{45}$$

Which leads to a constant Δr_p:

$$\Delta r_p = -\frac{\sqrt{\pi}\nu_t}{\eta v_k} \quad (St_{max} \gg 1). \tag{46}$$

Physically, this means that very big particles, which are barely affected by the surrounding gas wind or turbulence, stay where they are formed.

4.3 Gas Background

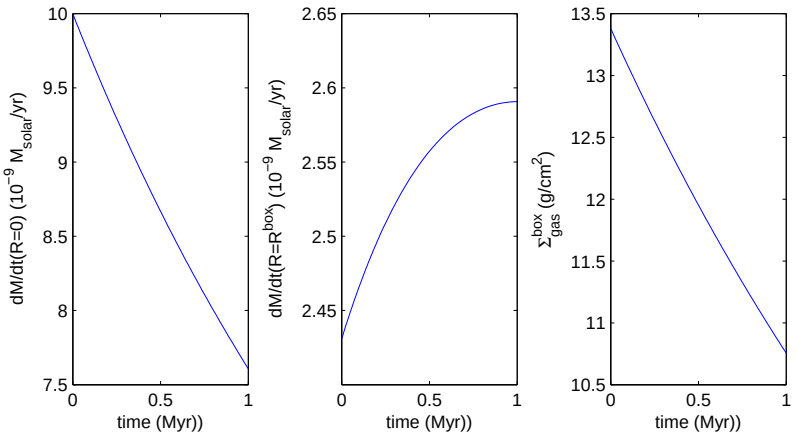

Figure 3: The evolution of gas background: accretion rate of gas at $r = 0$ (*left*) and $r = r_{box}$ (*middle*), and the gas surface density $\Sigma_g(r = r_{box})$ (*right*).

Figure 3 shows the properties of the gas background in the self similar solution of disk evolution, which shows no significant change over the $1Myr$ timescale. The surface density in the 'box' is about 10 times larger than the surface density used in the simulation of Zhu et al 2011. The accretion rate at $r = r_{box}$ is generally one order of magnitude less than the accretion rate into the central star.

4.4 Dust Depletion

The metallicity in the outflow is significantly reduced in the fiducial model due to two effects: filtration of the big particles and particle growth. In

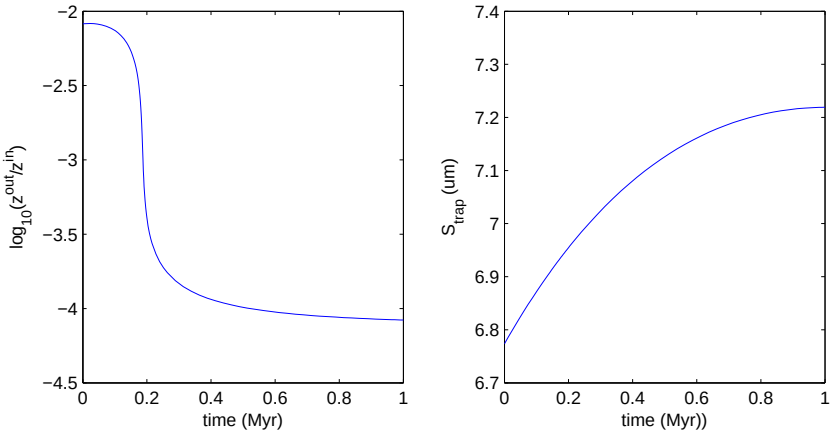

Figure 4: The depletion of metallicity in the outflow gas relative to the inflow gas Z^{out}/Z^{in} (*left*) and the evolution of s_{trap} (*right*).

Figure 4, the filtration effect causes an initial depletion by a factor of $\sqrt{s_{trap}/s_{max}} \sim 10^{-2}$. As the particle grow, most of the mass in the small particles coagulate into the bigger ones, leading to a depletion by a factor of another 2 orders of magnitude.

5 Parameter Search

This simple model enables us to easily search in the parameter space and probe more into this problem. We looked at the relatively uncertain parameter of sticking efficiency ϵ, turbulent parameter α_t, and the planet position r_{planet}.

5.1 Sticking Efficiency

The sticking efficiency ϵ is the most uncertain parameter in this model, which can be seen as the average sticking efficiency of the biggest particle colliding with others over all size and relative velocity range. From equation (42), the growth rate of the particle is proportional to ϵ. As shown in figure 5, in order to get a significant effect of particle growth and dust depletion, we need $\epsilon \gtrsim 10^{-2}$.

5.2 Turbulent Parameter

Figure 6 shows that the growth rate of particles is relatively insensitive to the turbulent parameter. However, the dust depletion is smaller for more turbulent disk, because stronger turbulence lead to weaker concentration

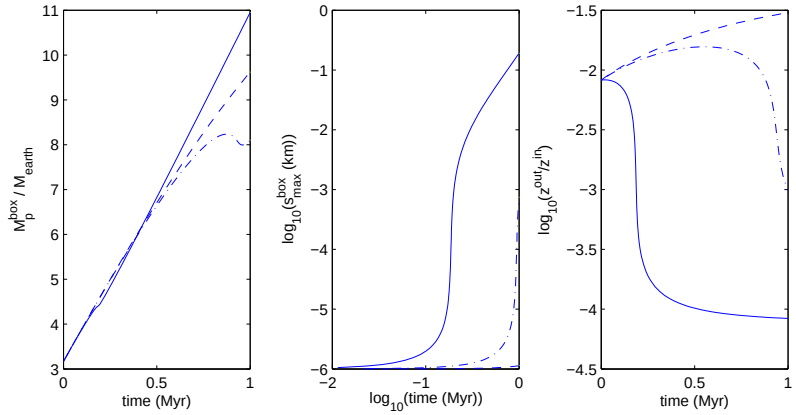

Figure 5: Particle mass M_p^{box} (*left*) and maximum particle size s_{max}^{box} (*middle*) in the box and dust depletion Z^{out}/Z^{in} (*right*) for $\epsilon = 10^{-3}$ (*dashed*), $\epsilon = 10^{-2}$ (*dotted dash*) and $\epsilon = 10^{-1}$ (*solid*)

effect of particles, and the increase of Δr_p in equation (44) results in a bigger Z^{out}.

5.3 Planet Radius

As can be seen in figure 7, the planet position, or the radial location of the edge of the gap, has a significant effect on the growth rate of particles. For a closer-in planet, the particles can grow to a bigger size, simply because there is more material in the inner disk.

6 Conclusion and Discussion

6.1 Transitional and Pre-transitional Disks

In this paper we have studied the dust evolution at the edge of the gap opened by a giant planet in the gas disk, showing that the effect of filtration and particle growth leads to a reduction of the particle flow by 2-4 orders of magnitude, which provides excellent agreement with observational data. We thus suggest that the presence of multiple gas giants is not necessary for the formation of the transitional disk. For the pre-transitional disk, there are two possible explanation for their optically thick inner disk: 1. The pre-transitional disk may be a former stage of the transitional disk, with the dust in the inner hole not yet cleaned by accretion and dust migration. This should also lead to the effect that the gap in the transitional disk is clearer than the pre-transitional disk. 2. The particles are trapped in the inner disk, possibly due to the presence of another gas giant.

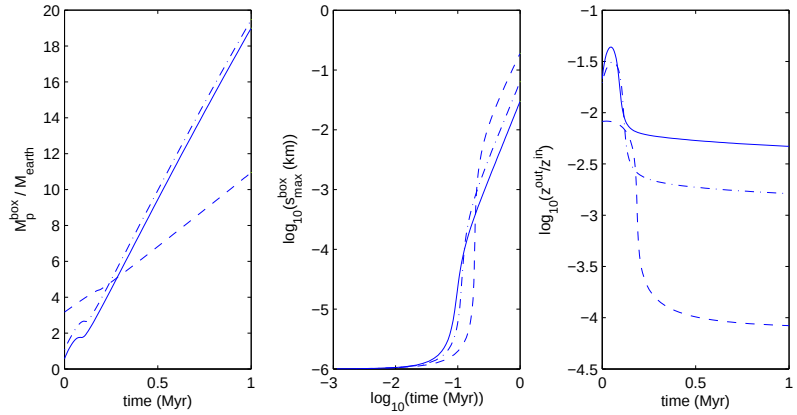

Figure 6: Particle mass M_p^{box} (*left*) and maximum particle size s_{max}^{box} (*middle*) in the box and dust depletion Z^{out}/Z^{in} (*right*) for $\alpha_t = 0.001$ (*dashed*), $\alpha_t = 0.005$ (*dotted dash*) and $\epsilon = 0.01$ (*solid*)

The essential requirement for the filtration effect is the presence of a local pressure maximum in the gas disk. Here we looked at the gap formed by a giant planet, but in principle, the pressure maximum could be induced by other mechanisms, such as the snow line or a dead zone, which could also act like a filter and give rise to similar effects.

6.2 Outlook on Planet Formation

Two problems have long been existing in the standard theory of planet formation: 1. There is a size barrier of particles growth of $1m$ for which the inward migration is much faster than the particle growth. 2. The timescale for the core formation of gas giants is significantly longer than the lifetime of protoplanetary disk. By trapping particles and forming a local density increase of solids at the gap edge, we showed that the particles can grow into kilometer sized planetesimals in a timescale of $1Myr$ at a radius of tens of AU. This provides a favorable place for the formation of planets beyond the orbit of a gas giant.

For the formation of planets from planetesimals, the particle-particle and particle-gas gravitational interaction becomes equivalently important as the particle interaction with the gas. This is beyond the consideration of our paper, and more realistic models such as N-body simulation are required.

References

[1] Espaillat et al. 2007 *The Astrophysical Journal, 664: L111L114*

[2] Espaillat et al. 2010 *The Astrophysical Journal, 717:441457*

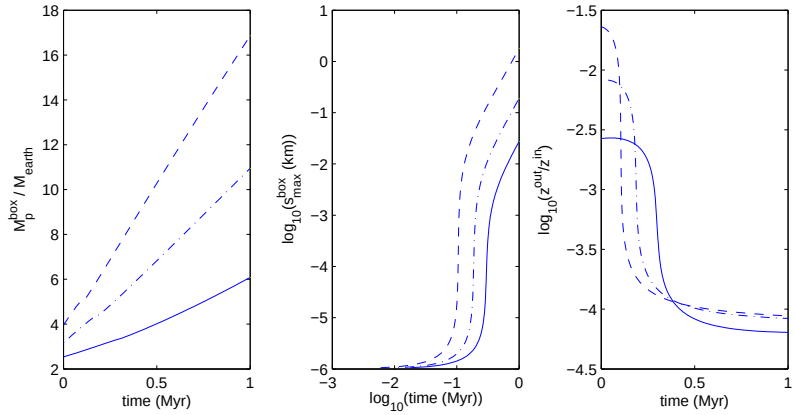

Figure 7: Particle mass M_p^{box} $(left)$ and maximum particle size s_{max}^{box} $(middle)$ in the box and dust depletion Z^{out}/Z^{in} $(right)$ for $r_{planet} = 20AU$ $(dashed)$, $r_{planet} = 30AU$ $(dotted\ dash)$ and $r_{planet} = 40$ $(solid)$

[3] Zhu et al. 2011 *The Astrophysical Journal, 729:47 (12pp)*

[4] Alexander & Armitage 2007 *Mon. Not. R. Astron. Soc. 375, 500512*

[5] Alexander & Armitage 2009 *The Astrophysical Journal, 704:9891001*

[6] Rice et al. 2006 *Mon. Not. R. Astron. Soc. 373, 16191626*

[7] Garaud 2007 *The Astrophysical Journal, 671:20912114*

[8] Hartmann et al. 1998 *The Astrophysical Journal, 495 : 385400*

[9] Weidenschilling 1977 *1977Ap&SS..51..153W*